

## New Visual Tools for Rhythmic Partitioning Analysis of Musical Texture

*Novas ferramentas visuais para a análise de particionamento rítmico da textura musical*

**Marcos da Silva Sampaio**

*Universidade Federal da Bahia*

**Pauxy Gentil-Nunes**

*Universidade Federal do Rio de Janeiro*

**Vicente Sanches de Oliveira**

**Sidnei Marques de Oliveira**

**Jaderson Cardona de Oliveira**

*Universidade Federal da Bahia*

**Abstract:** The *Partitional Theory of Musical Texture* provides a graphical tool, the *partitiogram*, to show relations between textural partitions. Despite its great utility, the *partitiogram* does not identify the occurrence frequency of each partition in a piece. In this paper, we propose two new *partitiograms* to represent partitions' occurrence frequency and to show partitions' differences among the sections of a given piece. The proposed tools made it possible to identify relevant aspects of the texture in nine analyzed works.

**Keywords:** Musical Analysis. Systematic Musicology. Computational Musicology. Partitional Theory.

**Resumo:** A *Teoria Particional da Textura Musical* dispõe do *particiograma*, uma ferramenta gráfica que mostra as relações entre partições texturais. Apesar da sua grande utilidade, o *particiograma* não identifica a frequência de ocorrência de cada partição da peça. Propomos dois novos *particiogramas* para representar a frequência de ocorrência das partições, e para mostrar as diferenças de partições entre seções de uma dada obra. As ferramentas propostas possibilitam a identificação de aspectos relevantes da textura em 9 obras analisadas.

**Palavras-chave:** Análise Musical. Musicologia Sistemática. Musicologia Computacional. Teoria das Partições.



## 1. Introduction

The Partitional Analysis of Musical Texture (PA) by Pauxy Gentil-Nunes (Gentil-Nunes and Carvalho 2004; Gentil-Nunes 2009) has two graphic tools for visualizing textural configurations and texture behavior throughout a musical work: the *partitiogram* and the *indexogram* (Gentil-Nunes 2009, pp. 33–61). Such tools represent, in different ways, the *agglomeration* and *dispersion* indices of the rhythmic partitioning of the texture of a composition.<sup>1</sup>

The partitiogram is a scatter plot with agglomeration and dispersion values of each partition<sup>2</sup> on the x- and y- axes, respectively (Gentil-Nunes 2009, p. 40). This chart allows identifying textural characteristics of the partitions by the dots' position in the graphic area. For example, textures with partitions near the x-axis have a unified sound that is more massive as the x-dimension is raised to the right side and more polyphonic and complex as their position stands close to the y-axis and in higher positions.

As an example, two excerpts are shown in Fig. 1. The first one (Fig. 1a) alternates between the violin solo, partition (1), and blocks articulated by all strings, partition (4). In this case, the two employed partitions have a common feature: they are composed of a single, homorhythmic element or block (composed, in this case by 1 or 4 simultaneous notes). In the second example (Fig. 1b), on the other side, all partitions are constituted by multiple independent elements, bringing a more polyphonic character to the music. In this way, a more scattered and fast distribution of segments is attributed to each partition than the former example, where their progression is rhythmically regular.

Naturally, these features can be observed directly in the score, but finer conclusions can be drawn from these graphical arrangements and correlations. For instance, there is a partial relation of complementation between the contrasting excerpts of Fig. 1, as the partition sets of the two examples are disjoint. To fulfill all possible partitions of four sounding components, it would

---

<sup>1</sup> The agglomeration and dispersion indices result from simple counting of pairwise relations between the individual components of a textural configuration (for example, musicians, instrumental parts, or sections). This distinction is made considering the qualities of collaboration, convergence, or congruence, for agglomeration, and contraposition, divergence, or incongruence, for dispersion.

<sup>2</sup> In the present paper, we will always use the word *partition* as synonymous with *textural configuration*; see details in Section 2.

be enough to add partitions (2) and (3) to the union of sets. This will be the case for the musical remainder of both quartets, as all partitions of 4 and, eventually, more oversized configurations derived from double stops are expected to be used in a piece dedicated to this instrumental group.

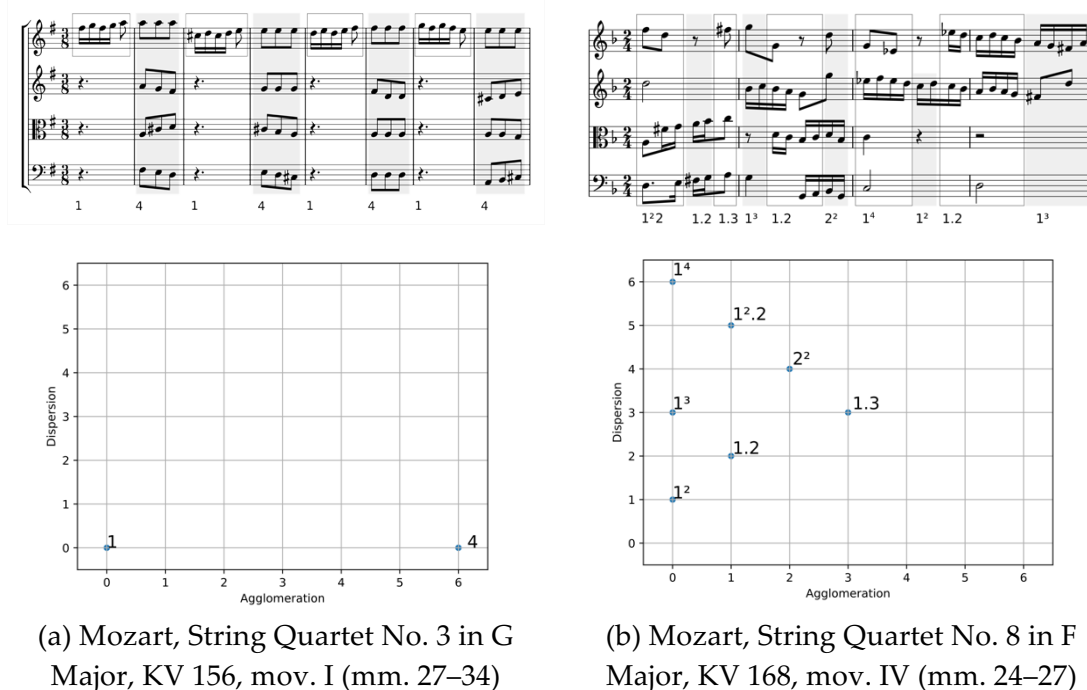


**Figure 1:** Annotated scores with partitions and simple partitograms of two excerpts from Mozart’s String Quartets. Generated by Music21 (Cuthbert and Ariza 2010), and RP Scripts (Sampaio and Gentil-Nunes 2022a, 2022b; see Section 4.2).

Despite the usefulness of the partitogram in quickly identifying the characteristics of a partition and comparing different partitions, in its original version, it is impossible to directly identify, through the graph, the relative number of occurrences of each textural partition in the music. This assessment is critical to evaluating the *referential partition*, an essential category for constructing one of the most active branches in the research of *PA* today - the *Partitional Complexes*.<sup>3</sup>

<sup>3</sup> For detailed information about the Partitional Complexes and the first approach to consider the frequency of partitions in a piece, see the work of Bernardo Ramos (2017, pp. 40–43) and Gentil-Nunes (2018).

For this reason, in this paper, we propose two new partitiograms. The first one is a *bubble chart*<sup>4</sup> where, beyond the plotting of the pair of *agglomeration* and *dispersion* indices ( $a$ ,  $d$ ), respectively in the x- and y-axes, there is a third dimension representing the frequency of occurrence of each partition. The second is the *Comparative Partitiogram*, where colored points represent partitions to assess the distinct features in each section of the pieces. Furthermore, we have implemented these partitiograms as a new RP Scripts functionality (Section 4.2).

We applied these visualizations to a corpus of nine pieces of different genres, analyzed the results, and discussed the problems and potential contribution of these visualizations to understanding a musical work's texture.

## 2. Rhythmic partitioning background

The formalization of musical texture, understood here as the interaction between constituent parts of a plot (or *texture-plot*, according to Fessel 2007), is a critical task in contemporary musical analysis. The pioneering work of Wallace Berry (1976, pp. 184–94) inspired several researchers to develop models to describe the relationships and transformations between textural configurations of pieces, especially in the context of concert music (Guigue 2009; Alves 2005).

*Partitional Analysis* (Gentil-Nunes and Carvalho 2004; Gentil-Nunes 2009) is one of the texture formalization initiatives developed through the mediation between Berry's work and the *Theory of Integer Partitions*<sup>5</sup> (Andrews 1984; Andrews and Eriksson 2004). Partitions are representations of integers by the sum of other integers. Since each integer has a finite set of partitions, it is possible to establish exhaustive taxonomies and map their relationships. One can, too, establish a biunivocal correspondence of the partitions with textural configurations. The inventory of textural configurations of a given instrumental set is called the *lexical set* in PA, and its cardinality is the *lexical sum*. A four-part ensemble (for example, a string quartet or a four-voice choir) has 11 settings in its lexical set:  $L = \{(1), (2), (1+1), (3), (1+2), (1+1+1), (4), (1+3), (2+2), (1+1+2), (1+1+1+1)\}$ .

<sup>4</sup> The term *bubble* is used here to express the type of graph. In PA, on the other side, the word *bubble* eventually indicates the geometric forms made by the agglomeration and dispersion indices ( $a$ ,  $d$ ) in the *indexogram* (Gentil-Nunes 2009, p. 53).

<sup>5</sup> The Mathematical Theory of Integer Partitions works exclusively in the domain of positive integers.

Each partition corresponds to a way of grouping and interacting between parts or musicians. Musical works written for this group can then be read as a continuous linear progression involving these 11 states. When a part activates, and others are suspended (with sustained durations arising from previous attacks), the common suspended state is considered as a situation of similarity or convergence and interpreted as an *agglomeration* relationship. This situation occurs, for instance, in Fig. 1b, third and fourth measures, generating the partitions ( $1^2$ ) and ( $1^3$ ).

Each configuration, or partition, has a specific degree of homorhythmic texture (that is, parts that articulate together) and polyphony (parts that articulate independently). This characteristic emerges from the qualitative evaluation of the *binary relationships* (i.e., pairwise assessments) between its elements, separating, on the one hand, the relationships of congruence, collaboration, or similarity; and on the other, the relations of incongruity, opposition, or difference. This count generates the *agglomeration* and *dispersion* indices, which form a pair (*a*, *d*). In the case of the texture-plot, the criteria are the attack points (in time-points) and the durations of each note. Other types of partitioning can be defined by different criteria, like structural nature of events (Fortes 2016); the performative relation between body and instrument (Ramos 2017); the instrumental sonic resources involved (Guigue and Santana 2018); compositional concepts and techniques (Moreira 2019), among others. For example, partition ( $2 + 2$ ) is more crowded than partition ( $1+1+1+1$ ), as its parts are more massive and the number of distinct parts is smaller; on the other hand, it is more dispersed than partition (4), the most crowded of the lexical set of density-number 4.<sup>6</sup>

The Partitiogram is a chart that presents the lexical set of a density-number with its partitions plotted from the indices (*a*, *d*). This representation makes it possible to evaluate the distances, the relationships between the partitions, and the more dispersed or clustered quality of set elements. Each piece of music covers a specific number of elements; therefore, the partitiogram can function as a global representation of the textural work developed. This functionality can be extended by comparing groups of distinct pieces, authors, and styles.

---

<sup>6</sup> The *density-number* is the absolute number of sounding components at a given time point (see Berry 1976, p. 185).

Regarding partitional notation, George Andrews (1984, pp. 1–2) abbreviates them with indices. The abbreviated notation for one repetition of a part such as  $(1+1)$  is  $(1^2)$ , for two repetitions such as  $(1+1+1)$  is  $(1^3)$ , and so on. For instance, the abbreviated notation of partition  $(1+1+1+1+2+2+2)$  is  $(1^4 2^3)$ .

Parsemat (Gentil-Nunes 2020) is a software devised to plot both graphs (indexogram and partitiogram). Moreover, it can do this task from MIDI and MAT files. In the present paper, we will propose carrying the functions to the Python environment, as well as some enhancements (mainly an occurring representation of the frequency of occurrences of a partition) and applications in a more extensive concert music repertoire.

### 3. New partitiograms

This paper proposes two new partitiograms: the *Bubble* and the *Comparative*. Both are upgrade proposals for the traditional partitiogram, bringing some information related to musical form and the relations between occurrences and frequency of partitions in the piece and in specific sections.

#### 3.1 Bubble Partitiogram

The *Bubble Partitiogram* is a bubble scatter chart representing agglomeration and dispersion values of each partition on the x- and y-axes and the percentual frequency of occurrence of each partition on the bubble sizes.

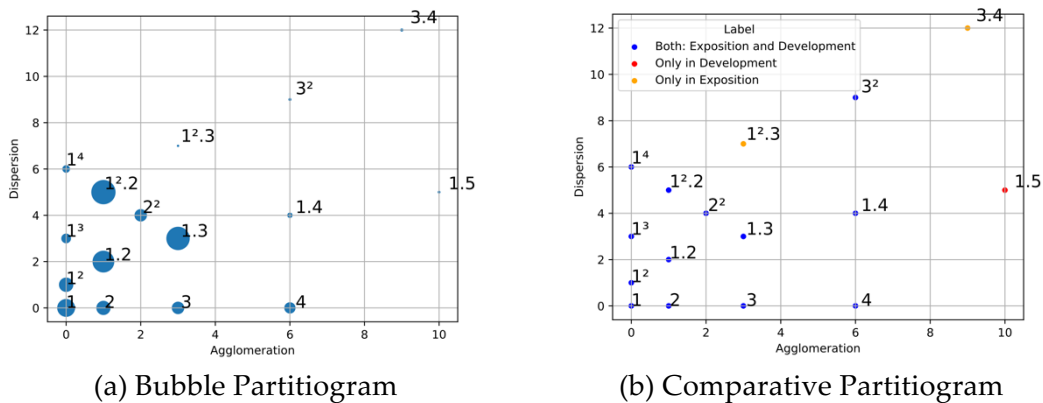


**Figure 2:** Mozart, String Quartet No. 19 in C Major, K. 465, *Dissonant* (1785/2001), mov. I. Partitiograms. Generated by RP Scripts (Sampaio and Gentil-Nunes 2022a, 2022b; see Section 4.2).

Fig. 2a shows the Bubble Partitiogram of Mozart's K. 465 String Quartet (Mozart 2001; see details in Section 5.2). The bubbles help to realize that partitions

with the highest values of aggregation and dispersion are rare, and the more frequent partitions have density-number from zero to four.

### 3.2 Comparative Partitiogram

The *Comparative Partitiogram* is a simple scatter chart, without bubbles, with the classification of events (partitions) by the musical section to which they belong. Three colors identify the events that belong to one, other, or both given sections. Fig. 2b shows the Comparative Partitiogram among exposition's and development's partitions of Mozart's K. 465 String Quartet (Mozart 2001; see details in Section 5.2). The colors help realize that most partitions occur in both sections and a few in one section. Partitions (1<sup>2</sup>3) and (3.4) appear only in exposition and (1.5) in development.

## 4. Methodology

This work's methodology comprises using computational routines to generate data and charts, running tests on a musical corpus, and analyzing and discussing results.

### 4.1 Corpus, repositories, and sources

We have selected a corpus of nine pieces from the *Common Practice Period* to verify the feasibility and usefulness of the tools. These pieces are musicologically relevant, available in digital scores in Kern or MusicXML format, and organized in the same musical form (Sonata), which is helpful for the standardization of comparisons.

The corpus consists of three piano sonatas, three string quartets, and three symphonies. Symphonies have the greatest potential for texture diversity due to the higher number of parts; quartets have the potential for comparison with each other due to instrumental equivalence; and piano sonatas have a slight limit in the potential for texture diversity due to the limitation of the fingers in the hand. Table 1 contains the information about the corpus and the repository that contains their digital score files (Beethoven 2004a, 2004b, 2015; Dvořák 2017; Grieg 2008; Haydn 2001, 2020; Mozart 2001, 2017).

The corpus' digital scores are available at Kern Scores (Sapp 2005a, 2005b) and MuseScore repositories (Musescore BVBA and others 2023). The Center for Computer Assisted Research in the Music (CCARH), part of Stanford University,



maintains Kern Scores. Their files are available in Kern format, suitable for processing by Humdrum toolkit (Huron 1995, 2022) and Music21 (Cuthbert and Ariza 2010, Cuthbert et al. 2010). Musescore's library is a collaborative repository that professionals and amateurs have extended. According to them, it is the largest library of musical scores available online.

Genre	Composer	Title	Mov.	Repository
Piano sonata	J. Haydn	Piano Sonata in E minor, Hob. XVI/34	1	MuseScore
Piano sonata	L. v. Beethoven	Piano Sonata No. 14 in C# minor Op. 27, No. 2	3	Kern Scores
Piano sonata	E. Grieg	Piano Sonata in E minor, Op. 7	1	Kern Scores
String Quartet	J. Haydn	Prussian String Quartet in B $\flat$ major, Op. 50 No. 1	1	Kern Scores
String Quartet	W. A. Mozart	String Quartet No. 19 in C Major, K. 465	1	Kern Scores
String Quartet	L. v. Beethoven	String Quartet No. 1 in F major, Op. 18, No. 1	1	Kern Scores
Symphony	W.A. Mozart	Symphony No. 41 in C major, K. 551	1	MuseScore
Symphony	L. v. Beethoven	Symphony No. 5 in C minor, Op. 67	1	MuseScore
Symphony	A. Dvorak	Symphony No. 9 in E minor, Op. 95, B. 178	1	MuseScore

**Table 1:** The analyzed corpus and its file origin

## 4.2 Tools

We have used RP Scripts (Sampaio & Gentil-Nunes 2022a, 2022b) to get the corpus rhythmic partitioning data, add form information labels, and plot all the charts. Furthermore, we have used Pandas (McKinney, 2010) and Music21 (Cuthbert & Ariza, 2010), two Python libraries (Van Rossum & Drake, 2009), to filter the data and plot scores of specific corpus excerpts.

This paper's data preparation consisted of four steps: 1) finding and fixing the digital scores' notation failures; 2) manually analyzing the pieces' form; 3) elaborating form label files; and 4) running RP Scripts. The manual analysis found pieces' section boundaries in terms of measure number and first beat offset.<sup>7</sup> The form label files are simple TXT files with sections' labels and their beginning locations (See Section 4.3).<sup>8</sup>

<sup>7</sup> Offset is Music21's term to define the distance between an event and the measure or piece beginning. For instance, in a quaternary metric, the first beat of a measure has offset zero, the second beat, offset one, and so on.

<sup>8</sup> CSV and TXT data files are available at <<https://github.com/msampaio/music-research-data/tree/master/rp-visual-tools/>> (Sampaio 2020).



## RP Scripts

RP Scripts consists of Python scripts to get rhythmic partitioning data from a digital score, plot multiple types of partitograms and indexograms, generate partition-annotated digital scores, and add form labels to these data. RP Scripts documentation is available on its webpage, and its application on music analysis is in Sampaio and Gentil-Nunes' paper (2022b). An important RP Scripts feature in this work is the location identification of partitions regarding measure number and offset.<sup>9</sup>

RPC script is the one responsible for the partitions' calculus. It outputs a CSV file with the structure in Table 2. RPL script reads a TXT file with form information (see Section 4.3). It adds this data to the CSV file. Finally, the RPP script generates the partitograms and indexograms charts.

Index	Measure number	Offset	Global Offset	Duration	Partition	Density-number	Agglom.	Dispers.	Label
96 + 0	96	0	192	1/2	(1 <sup>3</sup> )	3	0	3	Dev.
96 + 1/12	96	1/12	2305/12	1/2	(1 <sup>3</sup> )	3	0	3	Dev.
96 + 1/6	96	1/6	1153/6	1/2	(1 <sup>3</sup> )	3	0	3	Dev.
96 + 1/4	96	1/4	769/4	1/2	(1 <sup>3</sup> )	3	0	3	Dev.
96 + 1/3	96	1/3	577/3	1/2	(1 <sup>3</sup> )	3	0	3	Dev.
96 + 5/12	96	5/12	2309/12	1/2	(1 <sup>3</sup> )	3	0	3	Dev.
96 + 1/2	96	1/2	385/2	1/2	(1 <sup>3</sup> 3)	6	3	12	Dev.
96 + 7/12	96	7/12	2311/12	1/2	(1 <sup>3</sup> 3)	6	3	12	Dev.
96 + 2/3	96	2/3	578/3	1/2	(1 <sup>3</sup> 3)	6	3	12	Dev.
96 + 3/4	96	3/4	771/4	1/2	(1 <sup>3</sup> 3)	6	3	12	Dev.
96 + 5/6	96	5/6	1157/6	1/2	(1 <sup>3</sup> 3)	6	3	12	Dev.
96 + 11/12	96	11/12	2315/12	1/2	(1 <sup>3</sup> 3)	6	3	12	Dev.
96 + 1	96	1	193	1/2	(1 <sup>2</sup> 4)	6	6	9	Dev.
96 + 13/12	96	13/12	2317/12	1/2	(1 <sup>2</sup> 4)	6	6	9	Dev.
96 + 7/6	96	7/6	1159/6	1/2	(1 <sup>2</sup> 4)	6	6	9	Dev.
96 + 5/4	96	5/4	773/4	1/2	(1 <sup>2</sup> 4)	6	6	9	Dev.
96 + 4/3	96	4/3	580/3	1/2	(1 <sup>2</sup> 4)	6	6	9	Dev.
96 + 17/12	96	17/12	2321/12	1/2	(1 <sup>2</sup> 4)	6	6	9	Dev.

**Table 2:** Example of input data for partitogram plotting. Grieg, E. Piano Sonata in E minor, Op. 7 (1867/2008), mov. I, measure 96's first half. Generated by RP Scripts (Sampaio and Gentil-Nunes 2022a, 2022b).

Table 2 shows a snippet of Grieg's piano sonata data table generated by RPC script (converted here from CSV to table for better view). This table contains

<sup>9</sup> RP Scripts' operation is similar to Parsemat's.

events' location (measure number and local/global offset), partition, density-number, agglomeration and dispersion values of measure 96's first half (Fig. 3), and section name. The temporal distance between each pair of adjacent events is constant, based on the event minimum duration. For instance, a composition based on eighth notes ( $1/4$ ) and quarter-note triplets ( $1/3$ ) has a minimum duration of  $1/12$ . This choice allows the frequency analysis calculus of texture partitions.<sup>10</sup>



**Figure 3:** Grieg, E. Piano Sonata in E minor, Op. 7 (1867/2008), mov. I, mm. 95–96: Partition (1<sup>3</sup>3) and (1. 2. 3) in measure 96. Generated by Music21 (Cuthbert and Ariza 2010).

## Pandas

We have used Pandas to filter data by partition value and agglomeration/dispersion value intervals. The filter by partition helps find the location of a partition for posterior examination. For instance, we found partition (1. 2. 3) locations of Grieg's op. 7 with the following script.

```
import pandas
df = pandas.read_csv('grieg-op7.csv')
condition = df['Partition']=='1.2.3'
locations = df[condition]
print(locations)
```

The script's first line imports the Pandas library. The second converts Grieg's CSV file into a `pandas.DataFrame` object and stores it in the `df` variable. The third one tests the equality of all the `Partition` column's rows content and the given (1. 2. 3) value. Then it saves the result into the `condition` variable. The fourth line filters all the `DataFrame` rows where the condition of the previous line is true. The last line prints the results. This script found the (1. 2. 3) partition in

<sup>10</sup> Parsemat makes the reading of partitions at just the note attack points; these two strategies (note attack points or event minimum duration) both give the same results.

measures 96 (Fig. 3) and 108. Music21 library plots measures easily (see next section).

We also have used Pandas for data filtering by value interval. It helps generate data for a partitogram's region, simulating a zoom feature. For instance, the following script selects only the events with agglomeration and dispersion values lower than their medians.

```
import pandas
df = pandas.read_csv('file.csv')
a_col = df['Agglomeration']
d_col = df['Dispersion']
a_cond = a_col < a_col.median()
d_cond = d_col < d_col.median()
selection = df[a_cond & d_cond]
selection.to_csv('new-file.csv')
```

In this case, the operation `a_col.median()` returns the median of the agglomeration column and the operation `a_col < a_col.median()` returns True for all `a_col` rows lower than the column median and False otherwise. The `a_cond` variable stores the result of this conditional operation. The procedure is similar to the dispersion column. Finally, the operation `df[a_cond & d_cond]` concatenates agglomeration and dispersion conditions with the AND-type operator `&`, and the `to_csv` method saves the data into a new CSV file.

## Music21

We have used the Music21 library to generate music scores of notable passages for posterior examination. For instance, the following code imports the Music21 library transforms Grieg's digital score in Music21's data, extracts the measures 90 and 91, and plots them (Fig. 4).

```
import music21
score = music21.converter.parse('grieg-op7.krn')
measures = score.measures(90, 91)
measures.show()
```



**Figure 4:** Grieg, E. Piano Sonata in E minor, Op. 7 (1867/2008), mov. I, mm. 89–91.  
Generated by Music21 (Cuthbert and Ariza 2010).

### 4.3 New partitiograms' generation

In this paper, we introduce three new functionalities for RP Scripts: Bubble partitiogram; Comparative partitiogram; Rhythmic Partitioning Labeler script (RPL).

Both partitiograms utilize the available Rhythmic Partitioning Plotter script (RPP) structure. The new partitiograms extend the `AbstractPartitiogramPlotter` class with their specifications. The user can generate a Bubble partitiogram by passing the `-u` option in the RPP call (`python rpp.py -u file.csv`). Comparative partitiogram demands a previously labeled CSV file and the `-m` option in the RPP call (`python rpp.py -m labeled-file.csv`).

The user can also define multiple chart parameters, such as the partitiogram's dot size and the presence of partitions labels. RPP help describes these options (`python rpp.py -h`).

RPL script creates the labeled CSV file for the comparative partitiogram generation. It reads a TXT file with a label and its location per row. For instance, the annotation of Grieg's Op. Piano sonata's first movement is:

```
Exposition,1+0  
Development,82+0  
Recapitulation,130+0
```

RPL script adds these labels in a given CSV file generated by RPC (See Table 2) with this command line: `python rpl.py -c file.csv -t labels.txt`.

### 4.4 Data Analysis

The data analysis consisted of examining all pieces' partitiograms, identifying notable partitions, locating them in their data frames, plotting their musical score, and doing a contextual musical analysis. The partitiogram analysis consisted of examining clustering and scatter areas, bubble sizes, and locating detached partitions. The musical analysis consisted of understanding the partitions' locations in a formal context. For instance, some partitions appeared at the end of formal sections. We also did multiple visualization tests in this analysis process, such as bubbles inclusion in the Comparative Partitiograms, values transformation, and normalization of chart dimensions. These tests helped identify tools with more significant contribution potential to texture study.

## 5. Applied partitograms analysis

The partitogram bubbles allow us to perceive the partitions' occurrence frequency without an additional chart or table. The simultaneous observation of agglomeration, dispersion, and occurrence frequency has revealed some remarkable facts about the studied corpus, especially in the formal domain.

### 5.1 Piano Sonatas

The three analyzed piano sonatas are distinct in texture and length. Haydn's sonata has many passages in two voices and is the shorter one: a straightforward accompanied melody structure focused on the main line and with very sparing accompaniment (Fig. 5a).

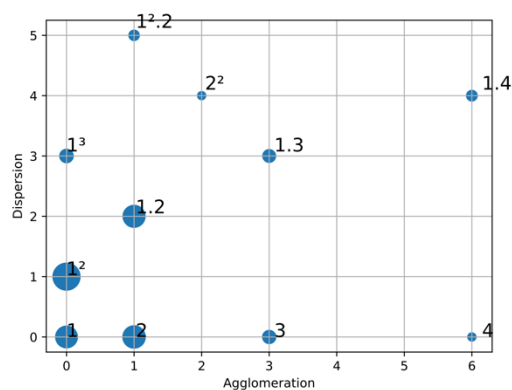
Beethoven's one has the highest chord frequency and is more extensive than Haydn's, also using more massive textures, prioritizing the instrumental effect, emphasizing attacks, and adding instrumental coloring effects (Fig. 5b). Grieg's has the highest diversity in counterpoint texture. In addition to Beethoven's artifices of emphasis, the composer brings a more complex texture, with more simultaneous elements in dialogue or even in polyphonic relation (Fig. 5c).

Harmonically, no new features come exclusively from the texture (for example, more complex harmonies). The difference in the cardinality of the blocks is produced more by doublings of sonorities that, on the whole, do not differ between the pieces by the number of chromas. The harmonic and tonal expansion in Beethoven and Grieg are caused by reasons other than texture.

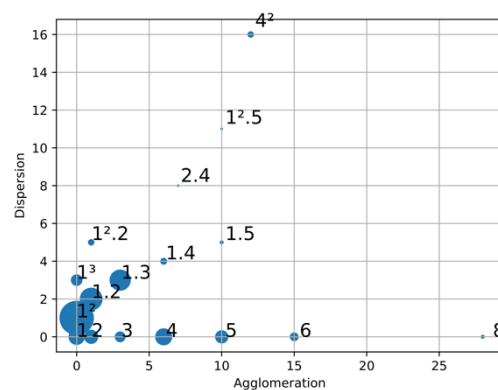
There is also no connection between the texture changes and the overall form, which are very similar, with idiosyncratic details that have no direct bearing on the differences in texture. This points out that texture can play an essential role in describing the contrast between styles, especially in the development of idiomatic writing for the instrument.

The partition's distribution of Haydn's sonata is well balanced. The occurrence frequency of partitions (2), (1<sup>2</sup>), (1.2), and (1.3) is slightly higher than the others (Fig. 5a). These partitions represent different types of texture: two-part homophony, two-part counterpoint, and accompanied melody, in a two-to-four-part writing. Comparing exposition and development, partitions (1<sup>2</sup>2), (2<sup>2</sup>), and (4) only occur in exposition, while partition (1.4) only happens in development. In the comparison between exposition and recapitulation, all

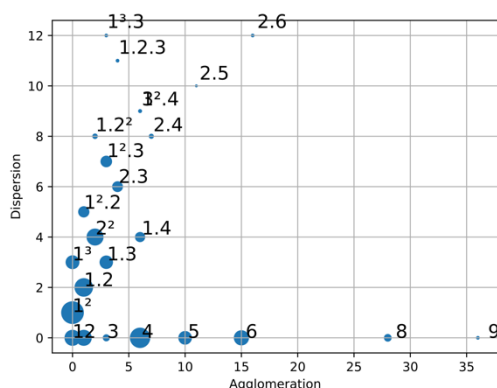
textures appear in both sections. The partitions ( $1^2$ ) and ( $2^2$ ) have the highest dispersion values in the piece.



(a) Haydn, J. Piano Sonata in E minor, Hob. XVI/34, L. 53 (1784/2020), mov. I



(b) Beethoven, L. v. Piano Sonata No. 14 in C# minor Op. 27, n. 2, *Moonlight* (1801/2004), mov. III

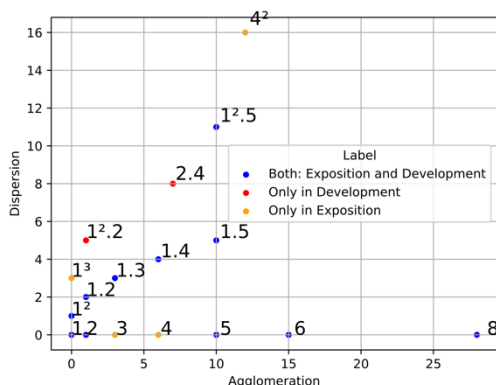


(c) Grieg, E. Piano Sonata in E minor, Op. 7 (1867/2008), mov. I

**Figure 5:** Piano sonatas: Bubble Partitiograms. Generated by RP Scripts (Sampaio and Gentil-Nunes 2022a, 2022b; see Section 4.2).

In Beethoven's sonata, most partitions have density-numbers from zero to five, highlighting the partition ( $1^2$ ) (two-part counterpoint, Fig. 5b). In addition to the significant agglomeration on five-part textures, there are partitions with density-number 8, such as (8) and ( $4^2$ ). In the exposition vs. development comparison, partitions unique to one section are more intermediate in agglomeration and dispersion values (Fig. 6a). For instance, partitions (3) and (4) are exclusive to exposition, while partitions ( $1^2$ ) and (2.4) are exclusive to development. The partition ( $4^2$ ) is the only highlight among the partitions that

belong solely to one section. It occurs at the end of the second theme, in measures 33, 37, 129, and 133 (Fig. 6b).



(a) Comparative Partitiogram: Exposition and Development. Generated by RP Scripts (Sampaio and Gentil-Nunes 2022a, 2022b; see Section 4.2).



(b) Partition ( $4^2$ ) in measure 33. Generated by Music21 (Cuthbert and Ariza 2010).

**Figure 6:** Beethoven, L. v. Piano Sonata No. 14 in C# minor Op. 27, n. 2, *Moonlight* (1801/2004), mov. III

As in Beethoven's sonata, in Grieg's sonata, most textures have a density-number from 1 to 5 (Fig. 5c). The most frequent partitions — ( $1^2$ ), ( $1.2$ ), (4), and even (5), (6), and ( $2^2$ ) — have well-balanced occurrence frequency at work. The most agglomerated partition has density-number 9. Compared to Haydn and Beethoven's sonatas, there is a great diversity of more dispersed textures, with up to 3 different rhythmic layers. There are five partitions of agglomeration and dispersion values more distant from the most: (9), ( $1^3$ ), ( $1.2.3$ ), and ( $2.5$ ).

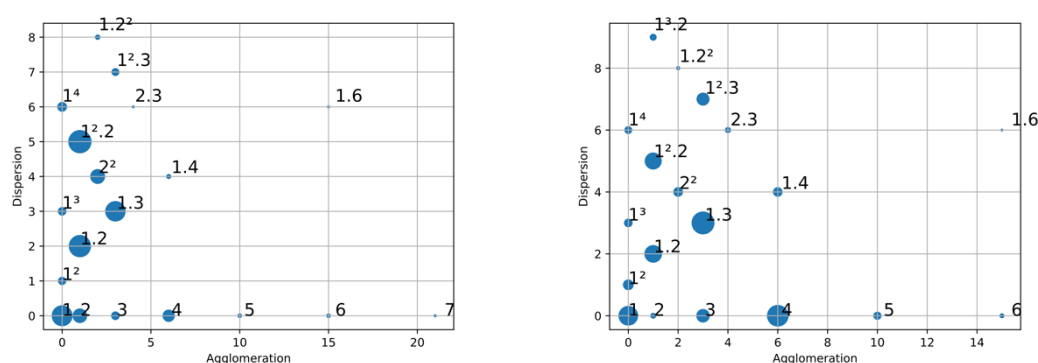
Concentrating the analysis on exposition and development, the two partitions with the highest dispersion value occur exclusively in development — ( $1^3$ ), and ( $1.2.3$ ). The partitions exclusive to exposition occur at intermediate points of the partitiogram. Partitions ( $1^3$ ) and ( $1.2.3$ ) occur in intermediate parts of the Development, in bars 96 and 108 (Fig. 3).

In comparing exposition and recapitulation, the partitions that appear only in one section occur at intermediate points of the partitiogram. Only partitions (9) and ( $2.5$ ) are worth mentioning, both of which are exclusive to the recapitulation. Partition (9) occurs on the piece's second-to-last chord (m. 228) and ( $2.5$ ) at the end of the second theme of the recapitulation.



## 5.2 String Quartets

In the three string quartets of the corpus, the prevalent partitions have density-number 4 — (4), (1.3), (2<sup>2</sup>), and (1<sup>2</sup>2), followed by partition (1.2) (Fig. 7a, Fig. 2b, and Fig. 7b). Unlike in Beethoven's quartet, partitions with a density-number higher than four are less frequent. It is not surprising since one- to four-part writing is expected in a string quartet ensemble.



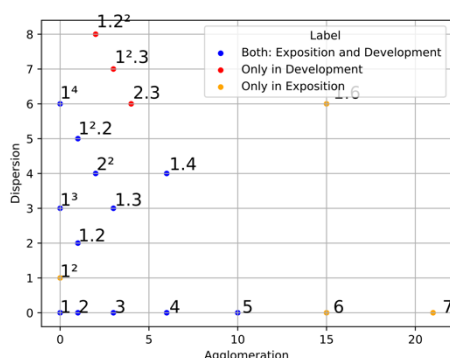
(a) Haydn, J. *Prussian* String Quartet in B♭ major, Op. 50 n. 1 (1809/2001), mov. I (b) Beethoven, L. String Quartet No. 1 in F major, Op. 18, n. 1 (1800/2004), mov. I

**Figure 7:** String quartets: Bubble Partitiograms. Generated by RP Scripts (Sampaio and Gentil-Nunes 2022a, 2022b; see Section 4.2).

In Haydn's quartet, considering the exposition and development sections, partitions (1.2<sup>2</sup>), (1<sup>2</sup>3), and (2.3), which have the piece's highest dispersion values, occur only in the development (Fig. 8a). On the other hand, partitions (1.6) and (7), which have the piece's highest values of agglomeration, appear only in the exposition. As such, in terms of the partition's occurrence frequency, the difference between the two sections lies in three more contrapuntal textures in development and two more massive sections in exposition.

Comparing exposition and recapitulation, partitions (1.6) and (7) only occur in exposition, and (1<sup>2</sup>3) only occurs in recapitulation. Partitions (1.6) and (7) happen in the exposition's first theme cadence, the most agglomerated point in the work (Fig. 8b). As the work does not have a retransition in the recapitulation, these partitions do not appear in this section. The most dispersed partitions, unique to the development section, occur in measures 63 and 66 (1.2<sup>2</sup>), 65 and 132 (1<sup>2</sup>3), and 63 and 89 (2.3). The most agglomerated partitions, exclusive to the exposition, occur in measures 26 (1.6), 60 (6), and 27 (7). These

marked differences between exposure and development show a direct connection between form and texture. See these partitions in Fig. 8c.



(a) Comparative Partitiogram. Exposition and Development. Generated by RP Scripts (Sampaio and Gentil-Nunes 2022a, 2022b; see Section 4.2).



(b) Mm. 25–28. Partition (1.6) in measure 26 and (7) in measure 27. Generated by Music21 (Cuthbert and Ariza 2010).




(c) Mm. 60–66. Partitions (1.6), (1.2<sup>2</sup>), and (2.3). Generated by Music21 (Cuthbert and Ariza 2010).


**Figure 8:** Haydn, J. *Prussian* String Quartet in B $\flat$  major, Op. 50 n. 1 (1809/2001),  
mov. I

Mozart's quartet has fewer partitions with high-value agglomeration than Haydn's quartet (Fig. 2a, and Fig. 7a), but it has two partitions, (3<sup>2</sup>) and (3.4) with higher dispersion values than Haydn's quartet. Although very different from the other sections in harmonic terms, the introduction does not contain any partition absent from the other sections, except for the coda, which does not have passages with a solo voice. When comparing exposition and development, only three partitions happen in only one section: (1.5) occurs only in development, and (1<sup>2</sup>3) and (3.4) appear only in exposition.

When comparing exposition and development, there are only three unique partitions: (1.5) only occurs in development, and (1<sup>2</sup>3) and (3.4) only appear in exposition (Fig. 2b). Partition (1.5), which has the work's highest agglomeration value, occurs at the development's final bar (Fig. 9a). Partition (3.4) appears in the second theme's first beat, right after a medial caesura (m. 56, See Fig. 9b). This partition does not occur in the recapitulation, where there is partition (3<sup>2</sup>) at this point. This difference is possibly due to the tonal-level adaptation, once the first violin has a quadruple-stop chord with low G in exposition, unfeasible in the recapitulation's key. On the other hand, partition (1<sup>2</sup>3) occurs in the second bar of the second theme.



(a) Mm. 153–156. Partition (1.5) in measure 154, before Recapitulation. Generated by Music21 (Cuthbert and Ariza 2010).

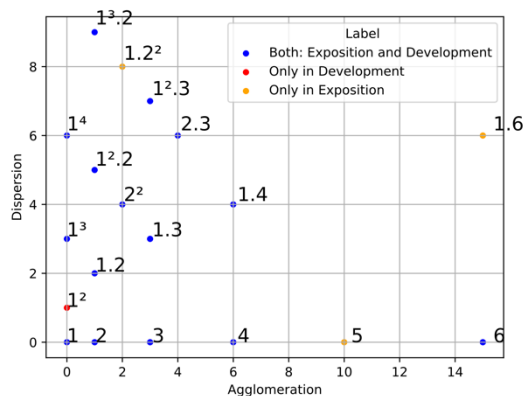


(b) Mm. 55–56. Partition (3.4) in measure 56, after Medial Caesura (MC). Generated by Music21 (Cuthbert and Ariza 2010).

**Figure 9:** Mozart, W. A. String Quartet No. 19 in C Major, K 465, *Dissonant* (1785/2001), mov. I

Beethoven's quartet has a much more expressive use of partitions of density-number 5 — (5), (1.4), (2.3), (1<sup>2</sup>3), (1.2<sup>2</sup>), and (1<sup>3</sup>2), than Haydn's and Mozart's quartets. Partition (1.6), which has the piece's highest density-number, occurs only once, six measures before the development (m. 109, See Fig. 10a). Partition (6) appears at the end of the recapitulation (mm. 260–261) and in the piece's final measure (Fig. 10c).

In comparing the textures of exposition and development, the piece contains five partitions that solely appear in one section: (1<sup>2</sup>) occurs only in development, and partitions (1.2<sup>2</sup>), (5), and (1.6) appear only in exposition (Fig. 10a). In the comparison between exposition and recapitulation, three partitions solely belong to one section: (1.6) happens only in exposition, and (1<sup>2</sup>) and (6) occur only in recapitulation.



(a) Comparative Partitiogram. Exposition and Development. Generated by RP Scripts (Sampaio and Gentil-Nunes 2022a, 2022b; see Section 4.2).



(b) Mm. 108–109. Partition (1.6) in measure 109. Generated by Music21 (Cuthbert and Ariza 2010).



(c) Mm. 260–261. Partition (6) in measure 261. Generated by Music21 (Cuthbert and Ariza 2010).



(d) Mm. 55–64. Absence of partition (1<sup>2</sup>). Generated by Music21 (Cuthbert and Ariza 2010).



(e) Mm. 119–122. Two-part melodies among First theme fragments. Generated by Music21 (Cuthbert and Ariza 2010).

**Figure 10:** Beethoven, L. v. String Quartet No. 1 in F major, Op. 18, n. 1 (1800/2004), mov. I

Two-part counterpoint settings, partition  $(1^2)$ , occurs only in the development section (Fig. 10a). Observing the work in detail, one can see that, in the exposition, even when there are lagged entries of the same melodic material, as in the second theme (m. 55, Fig. 10d), the texture changes to three voices but never to two in counterpoint.

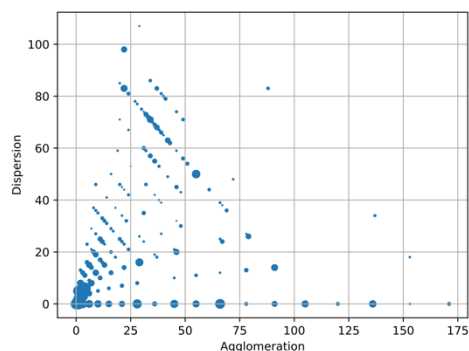
In the exposition, rests are used systematically in the first theme. In the presentations of fragments of the first theme in development, the space where there would be a rest is filled in with two-part melodies (e.g., mm. 119–122, Fig. 10e). These subtleties are perceived by observing the partitogram and verifying the location of each partition.

### 5.3 Symphonies

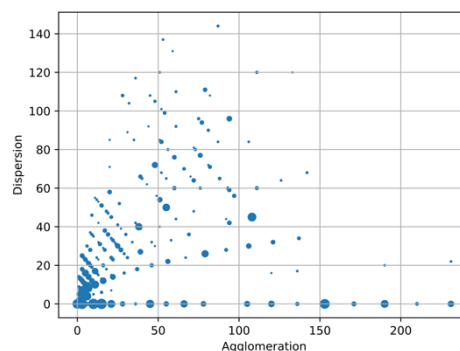
The partitograms of the three symphonies (Mozart, Beethoven, and Dvořák) have a significant concentration on partitions of low agglomeration and dispersion values (Fig. 11a–c). There is a slightly balanced frequency distribution, and some more frequent partitions.

In all three cases, the orchestra size directly impacts agglomeration's and dispersion's maximum values. Mozart's piece is for a smaller orchestra which results in the lowest maximum agglomeration and dispersion values; for instance, in Dvorak's piece, the large orchestra size is reflected in the partitions' agglomeration and dispersion of high values (Fig. 11c).

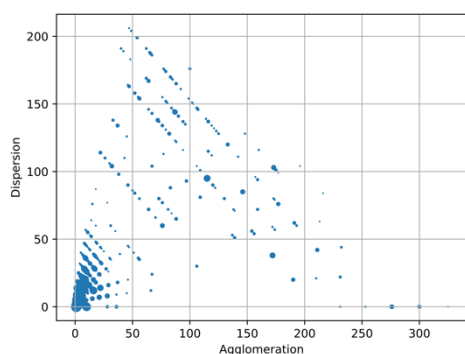
Mozart's symphony contains partitions of density-numbers up to 19 (Fig. 11a). There is a significant concentration up to density-number 6, the second clustering tier up to density-number 11, a slightly higher concentration of partitions of density-number 15, and sparse occurrences of partitions with densities between 12 and 19. The assessment of the partitogram indicates a particular prominence for partitions that represent a melody accompanied by a homophony sound —  $(1)$ ,  $(1^2)$ ,  $(1.2)$ ,  $(1.3)$ , ...,  $(1.14)$ ,  $(1.15)$  — and partitions with a dispersion value higher than the agglomeration's value. For instance, there is a diagonal with larger bubbles at density-number 15. Most of these bubbles correspond to *tutti*s that appear alternating with contrasting passages dedicated to the string section, mainly in the first theme, either in exposition or recapitulation. These string passages (with density-number 4) are eventually enriched with the addition of woodwind doublings, which sums up to density-number 5 or 6.



(a) Mozart, W. A. Symphony n. 41 in C major, K. 551, *Jupyter* (1788/2017), mov. I



(b) Beethoven, L. v. Symphony n. 5 in C minor, Op. 67 (1808/2015), mov. I



(c) Dvořák, A. Symphony No. 9 in E minor, Op. 95, B. 178, *New World* (1895),  
mov. I

**Figure 11:** Symphonies: Bubble Partitiograms. Generated by RP Scripts (Sampaio and Gentil-Nunes 2022a, 2022b; see Section 4.2).

Two points deserve attention in the comparisons, one with the highest agglomeration value, partition (19), and the other with the highest dispersion value, partition (3.4.5<sup>2</sup>). The latter occurs only in the exposition, at an intermediate point in the second theme (m. 87, see Fig. 12a), and (19) at the end of exposition (m. 120, see Fig. 12b) and in the coda, at the end of work (mm. 312–313). The exposition-development and exposition-recapitulation Comparative Partitiograms allow us to observe that partitions that only appear in one section solely fill the central spaces (Fig. 13a).

Beethoven's symphony contains many partitions of density-numbers up to 22 (Fig. 11a). There is a massive concentration of partitions with density-numbers up to eight and several partitions with some highlight, such as (18),

(20), (3.15), (2.13), (5.10), and (10). The partition with the highest density-number, (1.22), occurs only once, in the exposition, at the end of the first theme (m. 21, See Fig. 14). In this place, the contrast between the violin's part, with a duration that superimposes that of the *tutti* of the other 22 parts, is evident.

Figure 12 consists of two musical score excerpts, (a) and (b), from Mozart's Symphony n. 41. Excerpt (a) shows measures 86-88, with a partition (3.4.5) highlighted in measure 87. Excerpt (b) shows measures 119-120, with a partition (19) highlighted in measure 120. Both excerpts are generated by Music21 (Cuthbert and Ariza 2010).

(a) Mm. 86–88. Partition (3.4.5) in measure 87. Generated by Music21 (Cuthbert and Ariza 2010).

(b) Mm. 119–120. Partition (19) in measure 120. Generated by Music21 (Cuthbert and Ariza 2010).

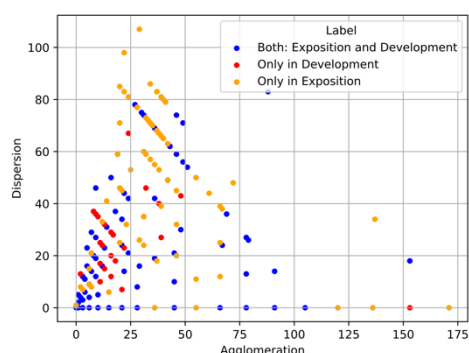
**Figure 12:** Mozart, W. A. Symphony n. 41 in C major, K. 551, *Jupiter* (1788/2017), mov. I

The Comparative Partitiograms of partitions from the exposition and development and exposition and recapitulation sections show that partitions that belongs solely to one section fill central voids (Fig. 13b). There are no situations as notable as in piano or string quartet works. There is a slight emphasis on partitions (4.6.12) and (10.12). Both occur at a development's intermediate point, at measures 168 and 169.

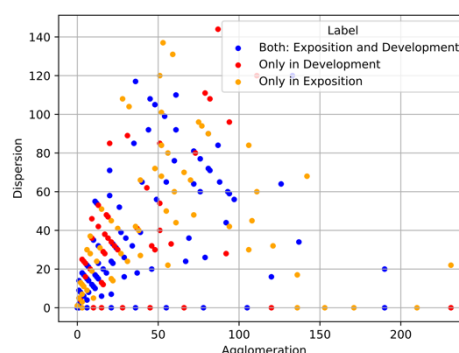
The partitions of Dvorak's symphony have density-numbers from zero to 26, with massive concentrations up to the value 12, and *concentration lines* with density-numbers 17, 21, 22, and 23 (Fig. 11c). Outside the region of the greatest



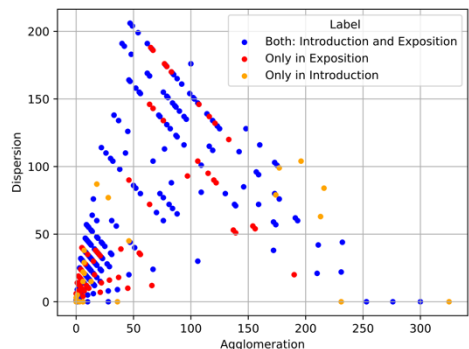
concentration, there is a slight emphasis on four partitions: (2.19), (5.17), (1.5.15), (1.2<sup>2</sup>19). Partition (26) occurs only once, at the introduction's final measure (m. 22). As with Mozart's and Beethoven's symphonies, partitions that appear solely in one section occur in a complementary way, filling the partitogram central spaces.



(a) Mozart, W. A. Symphony n. 41 in C major, K. 551, *Jupiter* (1788/2017), mov. I, Exposition and Development



(b) Beethoven, L. v. Symphony n. 5 in C minor, Op. 67 (1808/2015), mov. I, Exposition and Development



(c) Dvořák, A. Symphony No. 9 in E minor, Op. 95, B. 178, *New World* (1895), mov. I, Introduction and Exposition

**Figure 13:** Symphonies: Comparative Partitograms. Generated by RP Scripts (Sampaio and Gentil-Nunes 2022a, 2022b; see Section 4.2).

In comparing introduction and exposition partitions, there are several occurrences of accompanied melody partitions — (1.2), (1.3), (1.4), and so on). Except for partitions (1.2), (1.3), and (1.6), these partitions are absent from the introduction (Fig. 13c). Except for (1.2) passages, accompanied solo is less

frequent in the section. This particularity is also visible in the development section.

The image displays a musical score for Beethoven's Symphony No. 5, Movement I, measures 20-25. The score is in C minor, 2/4 time. It features a full orchestration with multiple staves. A specific measure (1.22) is highlighted, showing a transition in the music. The notation includes various musical symbols such as notes, rests, and dynamic markings.

**Figure 14:** Beethoven, L. v. Symphony n. 5 in C minor, Op. 67 (1808/2015), mov. I, mm. 20–25. Partition (1.22) in measure 21, before Transition. Generated by Music21 (Cuthbert and Ariza 2010).

Despite the hugeness of its orchestration, this piece keeps its textural configurations restricted to smaller ensembles, and *tuttis* are much less frequent than the other two pieces. In the respective partitiogram, the bubbles on the right are sparser and tinier, indicating less activity in this area.

## 6. Discussion

We gathered some partial conclusions about using computational tools to investigate musical texture from the data analysis on the works.

### 6.1 Relationships between partitioning attributes and musical form

We have noticed that partitions with a high agglomeration or dispersion value generally occur at formal segmentation points or in a position close to these points. It is worth noting the coincidence of the textures of greater density-number occurring at the end of the exposition's first theme of Beethoven's symphony and Haydn's and Beethoven's quartets.

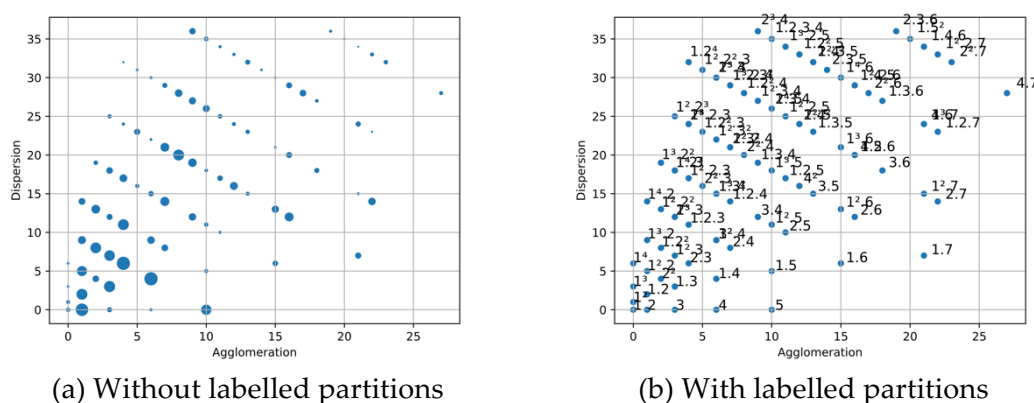


**Figure 15:** Dvořák, A. Symphony No. 9 in E minor, Op. 95, B. 178, *New World* (1895), mov. I. partitogram. Zoom in partitions with low-valued agglomeration/dispersion.

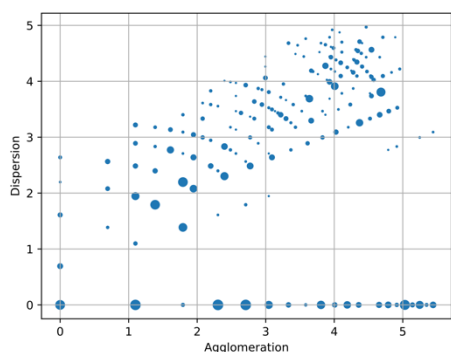
## 6.2 Quick view of relationships between partitiograms

Adapting the original Gentil-Nunes' partitogram preserves its qualities and adds the immediate perception of the frequency of the textural partitions. The Comparative Partitogram allows us to quickly identify the impact of texture on the difference between sections of a musical work. It can also be adapted to compare different works rather than sections.

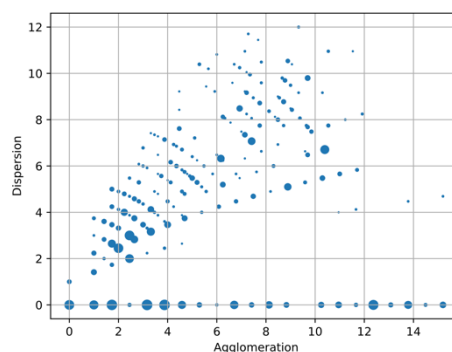
The Pandas library’s functionalities help define data filters to zoom in on specific parts of the partitogram, increasing its visualization power. For instance, Dvorak’s partitogram (Fig. 11c) has multiple crowded points in the low-valued agglomeration and dispersion area. Zooming this area improves the piece’s understanding (Fig. 15a).

### 6.3 Values transformations

Due to the quadratic growth of agglomeration and dispersion values, we tested transforming values before plotting to improve visualization. We applied logarithmic and square roots to each value before plotting. Logarithmic transformation inverted the chart, approaching higher values in crowded areas and moving lower values away, resulting in sparse areas. This transformation has improved lower values visualization (Fig. 16a). Square root transformation keeps the values more or less equidistant (Fig. 16b). Both operations have transformed diagonal lines that group the same density-numbers into concentric curves. This feature undesirably changes the relative positions between partitions, whose graphical structure is used in analytical applications to visually assess the quality of its relations. We concluded that the calculus method of agglomeration and dispersion values deserves an in-depth study, maybe with a final log or square root normalization to return more reliable values.



(a) Logarithmic transformed values.



(b) Square root transformed values.

**Figure 16:** Beethoven, L. v. Symphony n. 5 in C minor, Op. 67 (1808/2015), mov. I, transformed values

### 6.4 Comparison of pieces of distinct dimensions

Using axes with equal sizes in the partitogram comparison of distinct pieces can lead to a misguided interpretation. For instance, comparing a piano piece and a symphony with an equally dimensioned partitogram leads to the wrong idea that the symphony's piece is necessarily more diverse in partitions than the piano's one. There are 2713 possible partitions for a medium orchestra with 21 instruments (2222, 2221, timpani, strings) while 96 for a piano (limited by ten fingers). The possible piano partitions represent 3.5% of orchestra partitions.

Furthermore, the x-axis values of the orchestra's agglomeration should be from zero to 210, while the piano's one should be from zero to only 45. We conclude that the partitiogram is more helpful in comparing pieces with the same instrumental dimension. However, we must consider that a comparative assessment similar to the one adopted by Guigue (2009) – a mapping of partition indices values proportional to a maximum value relative to the full density number – can be tested in the future to evaluate partitiograms of pieces with distinct instrumental settings.

### 6.5 Labels on crowded partitiograms

Displaying partition labels in the charts with many dots makes them unreadable. However, its absence impairs the chart visualization. For instance, if zoomed in, Dvorak's partitiogram (Fig. 15a) is readable, but the absence of the labels impairs the chart comprehension. However, the labels' presence makes it unreadable (Fig. 15b). The solution to this problem is to improve the analyst interaction. One possibility is, for instance, to deploy a Javascript tool to exhibit dot labels on mouse hover. In this paper, we adopted a tedious procedure of zooming in partitiograms with `pandas.DataFrame` filters (see Section 4.2).

### 6.6 Problems

The digital files from both the KernScores and MuseScore repositories are not free of notation errors. Despite correcting the problems detected throughout this work, it is impossible to guarantee the absence of inaccuracies. Considering the number of events in the corpus, from 1500 to 43000 segments, we understand that punctual notation problems do not compromise the demonstrations of the partitiogram's usage.

In addition to the issue of sources, an ambiguous issue is dealing with unison and divisi. We only consider music notation in XML/Kern files and ignore the text annotations. Thus, we treat the unisons of instruments written on different staves as separate voices (e.g., Fl. I, II) and the ones in abbreviated textual form as *a 2* as a single voice. Thus, scores with different organization principles had slightly different results in calculating partitions. For further information see the concept of *threads*, developed by Daniel Moreira (2019, pp. 66–69).

## 7. Conclusions

In this paper, we have proposed Bubble and Comparison Partitiograms, presented analytical application on nine musical pieces, and discussed the results. We also have presented functionalities from Pandas and Music21 Python libraries. The representation of occurrence frequency on the Bubble Partitiogram helps comprehend the textural features of a piece once it allows immediate vision of frequent and rare piece partitions. The Comparison partitiogram is favorable for texture awareness regarding a formal context. In this regard, the proposed tools can help promote the information extraction of large musical corpora, one of the leading Music Information Retrieval (MIR) aims. Concerning the Partitional Analysis of Texture, we consider that the calculus method of agglomeration and dispersion values deserves further investigation to handle the growing distance among high-valued dispersion/agglomeration partitions. Finally, partitional analysis of some pieces has revealed connections between sparse partitions and form. In this way, we believe both Bubble and Comparative Partitiograms can be beneficial for the partitional analysis of texture.

## 8. Acknowledgements

This project is sponsored by Fundo de Amparo à Pesquisa do Estado da Bahia (FAPESB) and Universidade Federal da Bahia (UFBA).

## References

1. Alves, José Orlando. 2005. Invariâncias e disposições texturais: do planejamento composicional à reflexão sobre o processo criativo. Ph.D. Dissertation. Campinas: Universidade Estadual de Campinas.
2. Andrews, George. 1984. *The Theory of Partitions*. Cambridge: Cambridge University Press.
3. Andrews, George, and Kimmo Eriksson. 2004. *Integer Partitions*. Cambridge: Cambridge University Press.
4. Beethoven, Ludwig van. 2015. Symphony No. 5 in c Minor, Op. 67, 1st Movement (1808). In *Muscore BV*, edited by ClassicMan.
5. Beethoven, Ludwig van. 2004a. Piano Sonata No. 14 in c-Sharp Minor (Moonlight), Op. 27, No. 2. 3. Presto Agitato (1801). In *Kern Scores*, edited by Craig Sapp. Center for Computer Assisted Research in the Humanities at Stanford University.

6. Beethoven, Ludwig van. 2004b. String Quartet No. 1 in F Major, Op. 18, No. 1, 1. Allegro Con Brio (1800). In *Kern Scores*, edited by Craig Sapp. Center for Computer Assisted Research in the Humanities at Stanford University.
7. Berry, Wallace. 1976. *Structural Functions in Music*. New York: Dover Publications, Inc.
8. Cuthbert, Michael Scott; Ariza, Christopher. 2010. Music21 a Toolkit for Computer-Aided Musicology and Symbolic Music Data. In *Proceedings of International Symposium on Music Information Retrieval*, 637–42.
9. Cuthbert, Michael Scott; Ariza, Christopher; Hogue, Benjamin; OberHoltzer, Josiah Wolf. 2010. Music21: A Toolkit for Computer-aided Musicology and Symbolic Music Data. Internet site. Available on <<http://web.mit.edu/music21/>>. Accessed on Feb 10, 2023.
10. Dvořák, Antonín. 2017. Symphony No. 9 ("New World"), I - Adagio (1893). In *Musescore BV*, edited by Phil Ainsworth.
11. Fessel, Pablo. 2007. La doble génesis del concepto de textura musical. *Revista Eletrônica de Musicologia*, v. 11. Available at <[http://www.rem.ufpr.br/\\_REM/REMy11/05/05-fessel-textura.html](http://www.rem.ufpr.br/_REM/REMy11/05/05-fessel-textura.html)>.
12. Fortes, Rafael. 2016. Modelagem e particionamento de Unidades Musicais Sistêmicas. Master's Thesis, Universidade Federal do Rio de Janeiro.
13. Gentil-Nunes, Pauxy. 2009. Análise Particional: uma mediação entre composição musical e a Teoria Das Partições. Ph.D. Dissertation, Universidade Federal do Estado do Rio de Janeiro.
14. Gentil-Nunes, Pauxy. 2018. Nesting and Intersections Between Partitional Complexes. *MusMat: Brazilian Journal of Music and Mathematics*, v. 2, n. 1.
15. Gentil-Nunes, Pauxy. 2020. PARSEMAT: Parseme Toolbox Software Package V. 0.8 Beta. Available at <https://pauxy.net/parsemat-3/>. Accessed on Aug. 06, 2022.
16. Gentil-Nunes, Pauxy; Carvalho, Alexandre. 2004. Densidade e linearidade na configuração de texturas musicais. IV Colóquio de Pesquisa Do PPGM-UFRJ. *Anais...* Rio de Janeiro, pp. 40–49.
17. Grieg, Edvard. 2008. Piano Sonata in E Minor, Op. 7 (1867), 1. Allegro Moderato. In *Kern Scores*, edited by Craig Sapp. Center for Computer Assisted Research in the Humanities at Stanford University.
18. Guigue, Didier. 2009. *Esthétique de La Sonorité - L'héritage de Debussy Dans La Musique Pour Piano Du XXe Siècle*. Paris: L'Harmattan.



19. Guigue, Didier; Santana, Charles de Paiva. 2018. The Structural Function of Musical Texture: Towards a Computer-Assisted Analysis of Orchestration. Journées d'Informatique Musicale Jim 2018. In *Annales...* Amiens.
20. Haydn, Franz Joseph. 2020. Piano Sonata in E Minor Hob XVI/34 Movement I (1784). In *Muscore BV*, edited by Derek John Benton.
21. Haydn, Franz Joseph. 2001. String Quartet in B-Flat Major, Op. 50, No. 1, H III:44, 1 (1809). Allegro. In *Kern Scores*, edited by Frances Bennion and Craig Sapp. Center for Computer Assisted Research in the Humanities at Stanford University.
22. Huron, David. 2022. *Humdrum*. Internet site. Available on <<https://www.humdrum.org/>>. Accessed on Feb 10, 2023.
23. Huron, D. 1995. *The Humdrum Toolkit: Reference Manual*. Stanford, California: Center for Computer Assisted Research in the Humanities.
24. McKinney, Wes. 2023. *Pandas*. Internet site. Available on <<https://pandas.pydata.org/>>. Accessed on Feb 10, 2023.
25. Moreira, Daniel. 2019. Textural Design: A Compositional Theory for the Organization of Musical Texture. Ph.D. Dissertation, Universidade Federal do Rio de Janeiro.
26. Mozart, Wolfgang Amadeus. 2017. Symphony No. 41 - "Jupiter", K. 551 (1748). In *Muscore BV*, edited by Openscore.
27. Mozart, Wolfgang Amadeus. 2001. String Quartet No. 19 in c Major, "Dissonance", K 465 (1785), Adagio. In *Kern Scores*, edited by Frances Bennion and Craig Sapp. Center for Computer Assisted Research in the Humanities at Stanford University.
28. Muscore BVBA and others. 2023. *Muscore*. Internet site. Available on <<https://muscore.com/dashboard>>. Accessed on Feb 10, 2023.
29. Ramos, Bernardo. 2017. Análise de Textura Violonística: teoria e aplicação. Master's Thesis, Universidade Federal do Rio de Janeiro.
30. Sampaio, Marcos da Silva, and Gentil-Nunes, Pauxy. 2022a. *RP Scripts: Rhythmic Partitioning Scripts*, release 1.1. Available on <<https://github.com/msampaio/rpScripts>>. Accessed on Feb 23, 2023.
31. Sampaio, Marcos da Silva, and Gentil-Nunes, Pauxy. 2022b. Python Scripts for Rhythmic Partitioning Analysis. *MusMat: Brazilian Journal of Music and Mathematics* v. 6, n. 2.

32. Sampaio, Marcos da Silva. 2020. Music Research Data. Available on <<https://github.com/msampaio/music-research-data/>>. Accessed on Feb 23, 2023.
33. Sapp, Craig Stuart. 2005a. Online Database of Scores in the Humdrum File Format. International Society for Music Information Retrieval (ISMIR) 2005 Conference. *Proceedings...* Available at <<https://archives.ismir.net/ismir2005/paper/000123.pdf>>. Accessed on Feb 10, 2023.
34. Sapp, Craig Stuart. 2005b. *Kern Scores: A library of Virtual Musical Scores in the Humdrum \*\*kern Data Format*. Online library. Available on <<http://kern.ccarh.org/>>. Accessed on Feb 10, 2023.